

Optical methods for the evaluation of the thermal ionization barrier of lanthanide excited states in luminescent materials

M. Fasoli,^{1,*} A. Vedda,¹ E. Mihóková,² and M. Nikl²

¹*Dipartimento di Scienza dei Materiali, Università di Milano-Bicocca, via Cozzi, 53, 20125 Milano, Italy*

²*Institute of Physics, Academy of Sciences of the Czech Republic, v. v. i., Cukrovarnická 10, 16253 Prague, Czech Republic*

(Received 16 November 2011; revised manuscript received 9 January 2012; published 27 February 2012)

We improve a recently proposed approach for the evaluation of the thermal ionization barrier of the lanthanide excited states in luminescent materials by taking into account the effect of traps and their decay time temperature dependence. We present two distinct methods, and we apply them to the case of $\text{Lu}_2\text{Si}_2\text{O}_7:\text{Pr}$. To this purpose, wavelength resolved thermally stimulated luminescence and photoluminescence time decay measurements extending up to the ms time scale have been performed. In the frame of the first method, the thermal ionization barrier of the $\text{Pr}^{3+} 5d_1$ excited state has been evaluated by studying the progressive filling of traps during illumination by ultraviolet light within the $4f-5d_1$ absorption band of Pr^{3+} at different temperatures. The thermal ionization barrier turned out to be 0.54 ± 0.05 eV. In the second approach this parameter has been calculated by a numerical reconstruction of the temperature dependence of the $5d_1-4f$ delayed recombination decay integral in two different time windows ($[53.3 \mu\text{s} - 10.3 \text{ms}]$ and $[53.3 \mu\text{s} - 600 \text{s}]$) with the sum of contributions from different traps whose parameters have been investigated by thermally stimulated luminescence (TSL). The results obtained are in agreement with those found using the trap-filling method. The advantages and limits of both approaches have been critically exposed, in order to discuss the possibility of their extensive employment for the determination of the ionization barrier of a rare earth ion excited-state level in an insulating host.

DOI: [10.1103/PhysRevB.85.085127](https://doi.org/10.1103/PhysRevB.85.085127)

PACS number(s): 78.60.Kn, 78.70.Ps, 78.55.Hx, 61.72.-y

I. INTRODUCTION

Given the extensive use of rare earth (RE) ions as luminescence centers in phosphors and scintillators, determining the position of their ground and excited states level within the band gap of the host matrix is of crucial importance for the design and applications of these materials. Based on experimental values of charge transfer and $4f-5d$ transition energies of RE^{2+} ions, a model has been developed which provides their positions within the bandgap of an insulating host.¹ This model was extended to RE^{3+} ions as well with position uncertainties up to 0.5 eV¹ and later refined with the help of intervalence charge transfer transitions.² Different experimental techniques and methods have been insofar proposed and employed to determine particular transition energies, among these are optical absorption (OA), photoluminescence excitation (PLE),³ thermally stimulated luminescence (TSL),^{4,5} the microwave resonant cavity technique,⁶ photoconductivity (PC),⁷ and ultraviolet photoemission spectroscopy.⁸ PC in particular is a useful technique for determining how close to the conduction band (CB) the excited state of the luminescent ion is. When the energy difference is small enough, thermal ionization of an electron from the lanthanide excited state to the CB can occur even at room temperature (RT). As a consequence of this phenomenon the optical properties of the material can be adversely affected showing a luminescence quenching and a reduced light yield. Unfortunately, PC measurements can be performed only on bulk samples thus preventing the use of this technique on powder phosphors.

In this work we propose two different, purely optical, experimental methods for the evaluation of the thermal ionization barrier of the excited level of a luminescent center. Both these methods can be applied also on powder samples and rely on the effect of localized traps evidenced by TSL measurements.

In the presence of deep traps, which can be filled upon light illumination when thermal ionization of the RE ion excited level occurs, the thermal ionization barrier can be evaluated by monitoring the TSL intensity as a function of the illumination temperature. This method, which will be described first, involves only TSL measurements; it is relatively simple, but it requires the possibility to exploit traps stable in a conveniently wide temperature range.

The second method that will be described involves the parallel use of TSL and photoluminescence (PL) decay measurements. In a few recent works dealing with Ce^{3+} - and Pr^{3+} -doped orthosilicates,^{9,10} a new experimental approach was proposed, relying on purely optical techniques for the evaluation of the ionization barrier of the $5d_1$ level of Ce^{3+} (Pr^{3+}) governing the escape of the electron to the CB. When measuring the PL decay of Ce^{3+} (Pr^{3+}) at low temperature, the typical decay time of the $5d-4f$ transition, a few tens of ns, is observed. As temperature increases, however, thermal ionization of the $5d_1$ level may become effective. Such a process leads to PL decay-time shortening because of the onset of a second escape path, and it leaves an electron in the CB. The electron that escaped to the CB can thus be temporarily trapped in a localized defect and released at a later time, leading to a delayed radiative recombination process. By measuring the temperature dependence of the delayed recombination intensity, the authors calculate the ionization barrier of Ce^{3+} (Pr^{3+}) $5d_1$ excited state.

The delayed recombination intensity, however, is affected by the probability of captured electrons being released from the traps. Since this probability is temperature dependent, it can modulate the delayed recombination intensity and has to be taken into account for a reliable evaluation of the ionization barrier. We propose a mathematical model, relying on experimental TSL and PL data, which evaluates

the contribution of TSL traps to the delayed recombination as a function of temperature.

In this paper we apply both methods mentioned to Praseodymium-doped Lutetium pyrosilicate, $\text{Lu}_2\text{Si}_2\text{O}_7$ (LPS:Pr), calculating the ionization barrier of the $\text{Pr}^{3+} 5d_1$ excited state. LPS is an efficient inorganic scintillator, which shows particularly promising performance for medical application such as positron emission tomography.^{11,12}

We will present our results discussing the potentiality of the approaches together with the assumptions made and with the conditions for their fruitful application.

II. EXPERIMENTAL CONDITIONS

The LPS:Pr³⁺ single crystal considered in this work was grown in SIC CAS, Shanghai, China by the Czochralski method using an Ir crucible.¹³ The Pr³⁺ concentration in the melt was 0.5 at.%. For the measurements a plate of about $7 \times 7 \times 1$ mm was cut from the top of the parent boule with $\text{Ø}20 \times 40$ mm and polished to an optical grade. TSL measurements in the 10–310 K range were performed after x-ray irradiation at 10 K by a Philips 2274 x-ray tube operated at 20 kVp. The TSL apparatus consisted of a high-sensitivity spectrometer measuring the TSL intensity as a function of both the temperature and wavelength. The detection system was a monochromator TRIAX 180 Jobin-Yvon coupled to a charge-coupled-device detector Jobin-Yvon Spectrum One 3000 operating in the 190–1100 nm interval. The spectral resolution was about 5 nm. The TSL emission spectra were corrected for the spectral efficiency of the detection system. A 0.1 K/s heating rate was adopted.

TSL measurements were performed also after x-ray irradiation at RT. In this second case the measurements were obtained irradiating by a Machlett OEG 50 x-ray tube operated at 20 kV, and they were performed from RT up to 770 K with a linear heating rate of 1 K/s using two different apparatuses. The first apparatus used was a homemade high-sensitivity TSL spectrometer measuring the TSL intensity as a function of both temperature and emission wavelength; the detector was a double stage microchannel plate followed by a 512 diode array; the dispersive element was a 140 line/mm holographic grating, the detection range being 200–800 nm. The spectral resolution was approximately 15 nm. In the second TSL apparatus the total emitted light was detected as a function of temperature by photon counting using an EMI 9635 QB photomultiplier tube. In some cases, TSL glow curves were corrected for the temperature dependence of the $5d_1$ - $4f$ radiative transition of Pr³⁺.

PL measurements were performed by a custom-made 5000 M Horiba Jobin Yvon spectrofluorometer. PL-delayed recombination decays were excited by a microsecond xenon flashlamp and measured using the multichannel scaling method. An Oxford Instruments liquid nitrogen bath optical cryostat allowed the temperature regulation from about 190 to 500 K.

The decay fits were obtained by the least-square sum fitting procedure (SpectraSolve software package, Ames Photonics, Inc.) after performing the convolution of the considered function with the instrumental response. The PL-delayed

recombination intensity was measured after integration in a time window between 10 μs and 10 min.

III. RESULTS AND DISCUSSION

A. Method I (TSL)

The idea on which this method is based is quite straightforward: if a sample is exposed to optical radiation exciting selectively the luminescent centers, a fraction of the excited ions can be thermally ionized, and the electrons can become delocalized and migrate through the CB. For an electron situated in the excited state of a luminescent center, the probability $p(T)$ of being promoted to the CB is given by the expression

$$p(T) = e^{-\frac{E_{\text{th}}}{k_b T}}, \quad (1)$$

where k_b is the Boltzmann's constant, T is the absolute temperature of the sample, and E_{th} is the thermal ionization barrier. The ionized electrons can either recombine with a hole at a luminescent center or get trapped at localized defects. The probability of the release of an electron from the trap depends on both the temperature and characteristics of the trap itself. For some traps such a probability is not negligible and thus the electrons will be only temporarily trapped before returning to the CB. If we assume (i) that the fraction of thermally ionized electrons that is captured by a selected trap depends on neither temperature in a given temperature range nor light power (linearity of the trap response), and (ii) that the trap is stable (i.e., the electron release probability is negligible), then the intensity of the TSL peak related to that trap will be proportional to $p(T)$. Therefore, the fraction of thermally ionized electrons can be easily evaluated by means of the TSL technique. Then, by photoexciting the luminescent centers holding the sample at a given temperature, we can then evaluate, from expression (1), the thermal ionization barrier E_{th} .

The sample was mounted on a holder whose temperature was controlled by a Peltier cell within the range 283–353 K. Once the temperature was stable, the sample was exposed to 240 nm (band pass = 5 nm) light for 5 minutes, exciting the $4f$ - $5d_1$ transition of Pr³⁺ ions. The sample was then set to RT, and a TSL measurement was carried out from RT to 773 K. The glow curves obtained are reported in Fig. 1. At least three TSL peaks are detected from 350 to 650 K, while the signal above 650 K is due to deeper traps which are not fully emptied during subsequent TSL measurements.

The response linearity of the TSL signal was verified by TSL measurements obtained after x-ray irradiations at doses which gave rise to TSL intensities comparable to those obtained following light illumination (Fig. 1). It turned out that the signal between 430 and 490 K (related to the main TSL peak) displays a good linearity, while higher temperature peaks are supra-linear. Although, in principle, supra-linear peaks could also be employed provided that the correction for their response is performed, obviously in this case we preferred to exploit the main peak at 460 K. The integrals obtained from the glow curves of Fig. 1 from 430 to 490 K after subtracting the background signal are reported in the Arrhenius plot shown in Fig. 2. From the slope of the plot, the

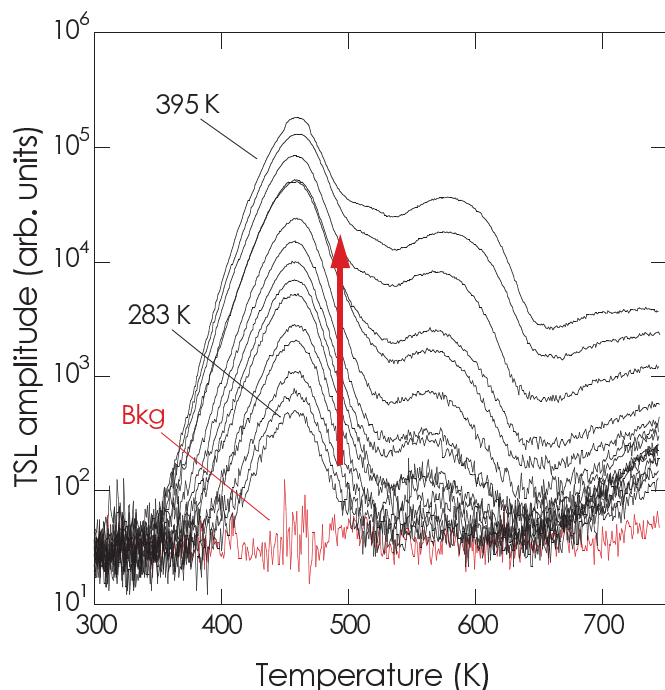


FIG. 1. (Color online) TSL glow curves of LPS:0.5mol%Pr after light illumination (240 nm, $630 \mu\text{W}/\text{cm}^2$) at different temperatures. The arrow indicates temperature increasing.

thermal ionization barrier E_{th} value was obtained, and it turned out to be 0.54 ± 0.05 eV. Finally, TSL measurements after excitation at different wavelengths (from 225 to 255 nm) were also performed. Since the shape of the TSL excitation spectrum so obtained was consistent with the optical $4f$ - $5d$ absorption

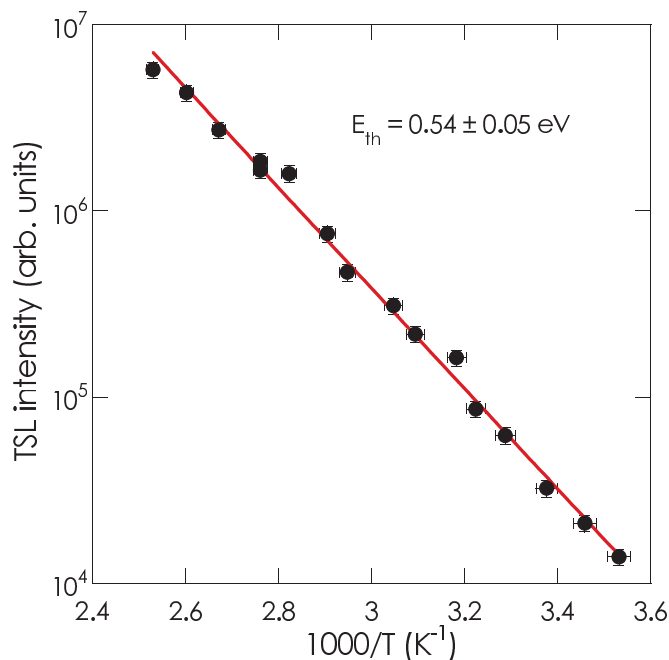


FIG. 2. (Color online) Arrhenius plot of the integrals obtained from the glow curves of Fig. 1 from 430 and 490 K after subtracting the background signal.

bands of Pr^{3+} , we can confirm that really the thermal ionization starts from the $5d_1$ Pr^{3+} excited level.

We observe that the main condition for application of this method is that the filling of traps from the excited state really involves the CB and no direct thermally assisted center-to-trap transitions occur. However in the latter case we would rather expect the filling of one specific trap. In our work we observed a variety of peaks following illumination, characterized by different thermal depths (see Table I of the next section); therefore, we believe that transition to CB is the most probably occurring mechanism.

B. Method II (PL/TSL)

In this approach we consider the temperature dependence of the luminescence center PL decay profile. When no ionization occurs, the intensity of the light emitted after the excitation pulse shows the decay profile characteristic of the luminescence center (faster if more recombination paths are present). In the case of Pr^{3+} $5d$ - $4f$ transition, for example, the decay time is in the order of a few tens of ns. If, on the other hand, a significant fraction of electrons gets thermally ionized, then delayed recombination can occur, giving rise to slower components in the decay curve.

As we already observed in Method I, after the excitation pulse, the fraction of excited centers that is thermally ionized is given by expression (1). Some of these ionized electrons will recombine immediately at the luminescence center with no delay so that it is not possible to discriminate between their emission and the one due to the prompt relaxation of photo-excited centers. A fraction of the ionized electrons, however, is temporarily trapped by localized defects. Such electrons, as a consequence, will undergo a delayed recombination at the luminescence centers. Thus this delayed recombination light holds the information about the thermally ionized electrons; analyzing with an appropriate model the temperature dependence of its intensity, we can extract the value of the thermal ionization barrier E_{th} . Similarly to what was explained for Method I, also in this case we assume that no direct thermally assisted center-to-trap transitions occur.

Being the delayed recombination light due to the effect of localized traps, let us first consider in our model, for simplicity, the case in which only one kind of trap is present. After the excitation pulse, the decay time profile of the delayed recombination light is governed by the decay time $\tau(T)$ of the traps, which are supplying the electrons to the luminescence centers. The emitted light intensity as a function of time, at temperature T , is given by the expression

$$I(t; T) = I_{0;T} e^{-\frac{t}{\tau(T)}}, \quad (2)$$

where $I_{0;T}$ is a constant proportional to the number of trapped electrons and $\tau(T)$ is the decay time of the traps that can be obtained from

$$\tau(T) = s^{-1} e^{\frac{E}{k_B T}}, \quad (3)$$

where E is the thermal depth of the trap and s is its frequency factor. Now let us assume that our detection system can integrate the light emitted within the time window $[t_1, t_2]$ after the excitation pulse. We remark that, since we are interested only in the delayed recombination light, it is important that

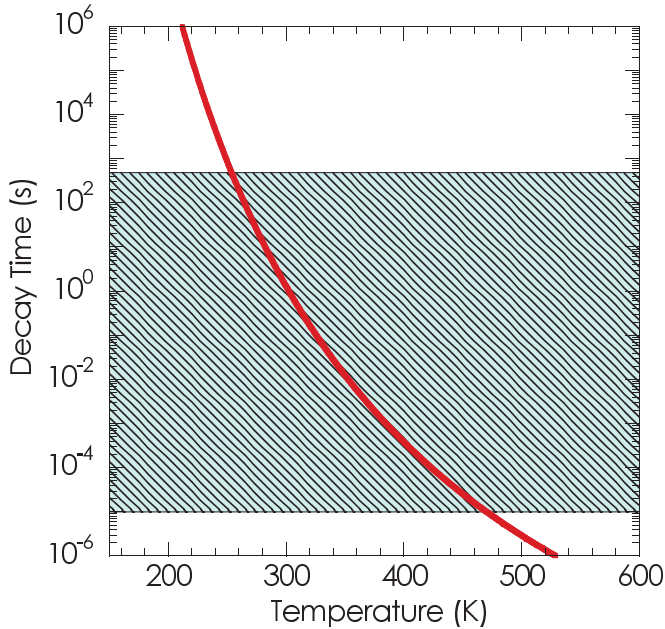


FIG. 3. (Color online) Temperature dependence of the decay time of a trap with depth $E = 0.84$ eV and a frequency factor $s = 1 \cdot 10^{14} \text{ s}^{-1}$. The dashed area indicates the time window $[t_1, t_2] = [10 \mu\text{s}, 600 \text{ s}]$.

the lower limit t_1 of the time window is high enough to avoid the prompt emission from being detected by our system. The delayed recombination intensity value $A_{\text{DR}}(T)$ that we obtain at temperature T is then given by

$$A_{\text{DR}}(T) = \int_{t_1}^{t_2} I(t; T) dt = I_{0;T} \tau(T) (e^{-\frac{t_1}{\tau(T)}} - e^{-\frac{t_2}{\tau(T)}}). \quad (4)$$

If we integrate expression (2) from 0 to ∞ we obtain the total delayed recombination light, that is

$$A_{\text{DR}}^{\infty}(T) = \int_0^{\infty} I(t; T) dt = I_{0;T} \tau(T). \quad (5)$$

This means that the fraction of the total delayed recombination light that is emitted within the time window $[t_1, t_2]$ and collected by the detection system is

$$\frac{A_{\text{DR}}(T)}{A_{\text{DR}}^{\infty}(T)} = (e^{-\frac{t_1}{\tau(T)}} - e^{-\frac{t_2}{\tau(T)}}). \quad (6)$$

As a realistic numerical example, let's consider a trap with a thermal depth $E = 0.84$ eV, a frequency factor $s = 1 \cdot 10^{14} \text{ s}^{-1}$, and a detection system integrating in the time window $[t_1, t_2] = [10 \mu\text{s}, 600 \text{ s}]$. The trap decay time can be calculated from expression (3), and its temperature dependence is plotted in Fig. 3. The shaded area indicates the region within the detection system time window, and it evidences that the trap decay time falls within the time window when the temperature is between approximately 250 K and 470 K.

Due to the strong temperature dependence of the trap decay time $\tau(T)$, the ratio in expression (6) is consequently also affected by temperature; this dependence is shown in Fig. 4.

From the plot it is evident that the ratio $A_{\text{DR}}/A_{\text{DR}}^{\infty}$ is close to 0 at any temperature except for the same temperature range in which the trap decay time falls within the time window $[t_1, t_2]$. The physical meaning of this curve is straightforward.

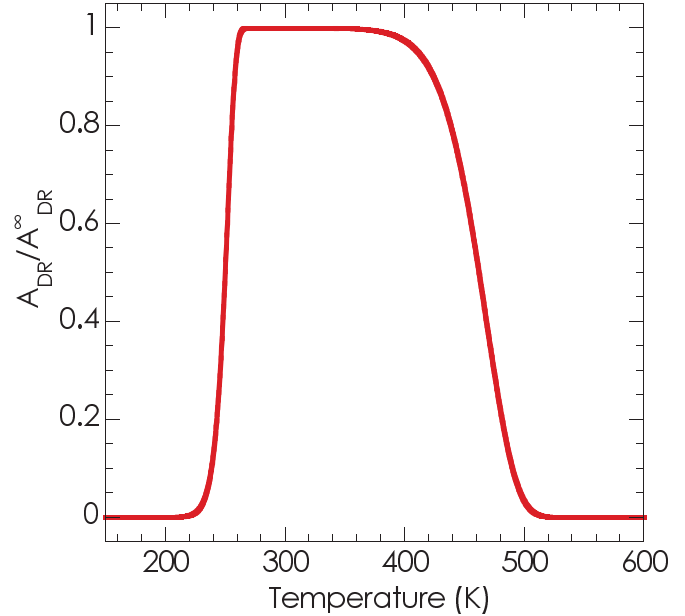


FIG. 4. (Color online) Temperature dependence of the fraction of delayed recombination light related to a trap with $E = 0.84$ eV and a frequency factor $s = 1 \cdot 10^{14} \text{ s}^{-1}$ emitted in the time window $[t_1, t_2] = [10 \mu\text{s}, 600 \text{ s}]$.

At high temperature (above 500 K), the trap decay time is so short that, after the excitation pulse, most of the trapped electrons are released (and recombine) in a time shorter than t_1 and cannot be detected. To the opposite limit, at any temperature lower than 250 K, the trap decay time is extremely long so that most of the delayed recombination light is emitted at longer times than t_2 . Only for intermediate temperatures a significant fraction of the light is detected. Following all these considerations, the intensity $I(T)$ of the delayed recombination light emitted in the time window $[t_1, t_2]$ is given by

$$I(T) = \text{const} \cdot e^{-\frac{E_{\text{th}}}{k_B T}} (e^{-\frac{t_1}{\tau(T)}} - e^{-\frac{t_2}{\tau(T)}}). \quad (7)$$

If we now extend the model to the case in which several trap species are involved, we need to sum the contribution of each trap to the delayed recombination light,

$$I(T) = \text{const} \cdot e^{-\frac{E_{\text{th}}}{k_B T}} \cdot \sum_i A_i (e^{-\frac{t_1}{\tau_i(T)}} - e^{-\frac{t_2}{\tau_i(T)}}), \quad (8)$$

where the index i runs through the different type of traps, and the constants A_i account for the different filling of the traps due to their different electron-capture probability. The temperature dependence of the decay time of each trap $\tau_i(T)$ can be calculated from experimental data obtained from TSL measurements. In fact the initial rise technique¹⁴ allows the evaluation of the thermal depth energy E_i of a trap and, if its recombination is of first order kinetics, also of its frequency factor s_i . The decay time of the trap at temperature T is then obtained from expression (3).

According to the model, the experimental procedure required to evaluate the thermal ionization barrier E_{th} can be summarized in three steps.

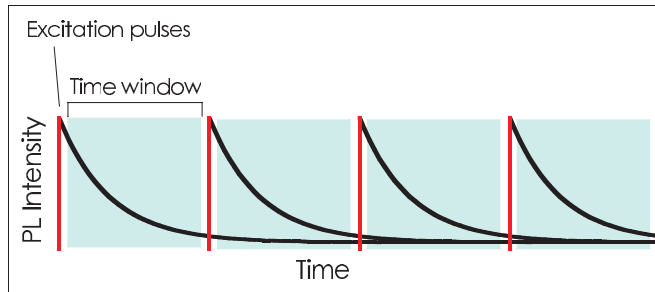


FIG. 5. (Color online) Sketch of the delayed recombination measurement.

(1) Measurement of the delayed recombination light intensity $I(T)$ integrating within the time window $[t_1, t_2]$ for a set of different temperatures T .

(2) Evaluation of the decay $\tau(T)$ for each trap from the trap energy depth E and its frequency factor s obtained from TSL analysis.

(3) Numerical fit of expression (8) to obtain the value of the desired parameter E_{th} .

Let's now apply the method to the case of LPS:Pr.

1. Step 1

The delayed recombination light intensity was monitored using conventional equipment for PL decay time measurements. The sample was excited in the $4f-5d_1$ absorption band (240 nm) of Pr^{3+} by a Xenon flashlamp (with a pulse width of about 3–4 μs and flash rate of approximately 10^2 Hz). The emission monochromator was set to 305 nm, close to the maximum of the $5d_1-4f$ emission. The detection was performed with the multichannel scaling method scanning the decay for approximately 10 ms. The system was set so that each excitation pulse (and corresponding measurement window opening) occurred immediately after the previous one so that nonmonitored intervals between successive time windows were due only to the dead time of the electronics (less than 100 μs). The measurement sequence is sketched in Fig. 5. The accumulation time for each measurement was 10 minutes. The measurement was performed at different temperatures in the range 197–497 K starting from the highest temperature.

In Fig. 6 some of the decay curves obtained are shown. It is important to notice that the time scale considered is several orders of magnitude longer than the characteristic decay time of the $5d_1-4f$ transition of Pr^{3+} (10 ms compared to tens of ns). A single channel covers 10.667 μs so that, apart from the first 4–5 channels containing the excitation pulse, all of the detected light is due to delayed recombination. We remark that the apparent increase of the background level (clearly visible in the channels before the excitation pulse) is due to delayed recombination light emitted at times longer than 10 ms and excited by previous pulses. The slow tails of the decays stack together increasing the background signal (see Fig. 5). As expected, this phenomenon is particularly evident for measurements performed at higher temperature where the thermal ionization of the excited level of Pr^{3+} is more effective. For the evaluation of the delayed recombination light we proceeded as follows. We first removed the first 4–5 channels containing the excitation pulse and the prompt

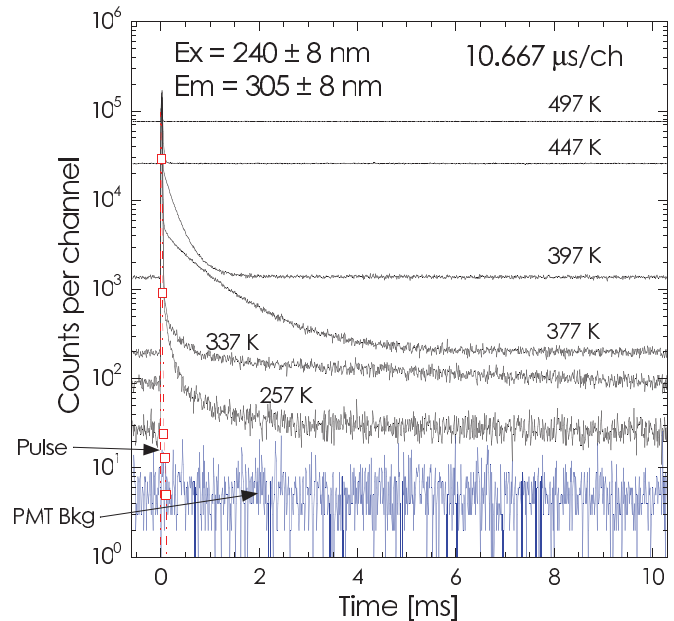


FIG. 6. (Color online) Delayed recombination curves performed on LPS:0.5mol%Pr at different temperatures under excitation of the $4f-5d_1$ transition of Pr^{3+} and monitoring the $5d_1-4f$ emission. The signal was accumulated for 600 s.

recombination light. Then we subtracted the background level detected in the channels before the pulse, and we integrated the curve in the whole time range (Fig. 7, grey area). The value obtained corresponds to an integration of the signal in the time window $[53 \mu\text{s}, 10.3 \text{ ms}]$. As a second option for the integration we subtracted the true photomultiplier background level integrating the signal marked by the dashed area in Fig. 7. This integration is approximately equivalent to collecting the delayed recombination light emitted during

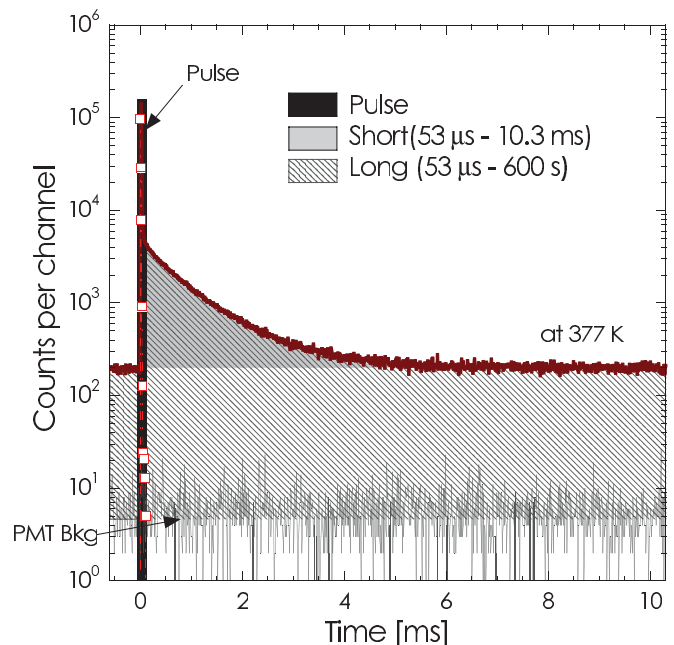


FIG. 7. (Color online) Example of the evaluation of the delayed recombination light emitted in two different time integration ranges.

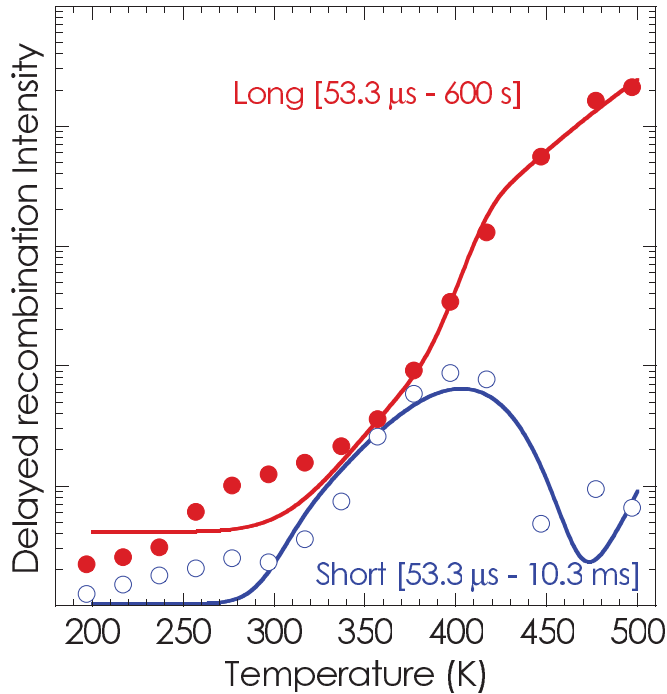


FIG. 8. (Color online) Temperature dependence of the delayed recombination light emitted by LPS:0.5mol%Pr in two different time integration ranges. The lines are numerical fits according to Eq. (8) with $E_{th} = 0.42$ eV for the short integration range and $E_{th} = 0.54$ eV for the long integration range. In the fits, we associated a statistical error to the data.

the whole measurement and corresponds to a time window [53 μ s, 600 s]. However, we are aware that this latter integration tends to underestimate the contribution of the slower decay components since the excitation pulses occurring toward the end of the measurements can contribute only to the fast components. Conversely, the short integration window is not affected by this problem, but data show a lower reliability due to the critical evaluation of the integral.

We will refer to the two different time integrations in the ranges [53 μ s, 10.3 ms] and [53 μ s, 600 s] as the “short” and “long” time windows, respectively. The intensity of the delayed recombination light emitted within both the short and long time window is reported as a function of temperature in Fig. 8. These curves were corrected for the temperature dependence of the PL efficiency of the Pr^{3+} $5d_1-4f$ emission measured in steady-state mode.

2. Step 2

We employed wavelength-resolved TSL measurements to identify which traps display emission in the $5d_1-4f$ transition of Pr^{3+} , which was selected for the PL-delayed recombination measurements. Figures 9–11 display the measurements performed both above (Figs. 9 and 10) and below (Fig. 11) RT. Above RT, we could compare the TSL patterns obtained after both light illumination and x-ray irradiation (Figs. 9 and 10, respectively): in the $5d_1-4f$ emission region up to 400 nm, we observed the same TSL peaks at 460 and 515 K (see Fig. 1) with different relative intensities. The emission of the highest T -peak in the 600 K region is centered at

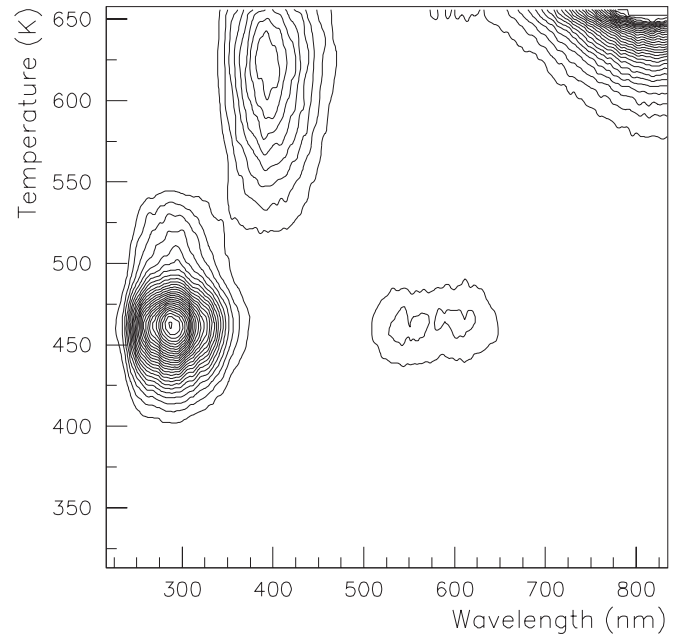


FIG. 9. Wavelength-resolved TSL measurements performed on LPS:0.5mol%Pr after RT 240 nm light irradiation.

400 nm; such emission is no longer due to Pr^{3+} , while it could be related to a defect. Therefore such a peak should not be considered in the numerical fit of expression (8) to be performed in Step 3. Analogous considerations can be made for the low T measurement: the only peaks emitting in the $5d_1-4f$ transition of Pr^{3+} are those at 77, 211, and 267 K.

We therefore evaluated the parameters of six traps responsible for peaks at 77, 211, 267, 334, 460, and 515 K by the “initial rise” method applied after suitable partial cleaning procedures of the glow curves coupled to numerical peak reconstruction

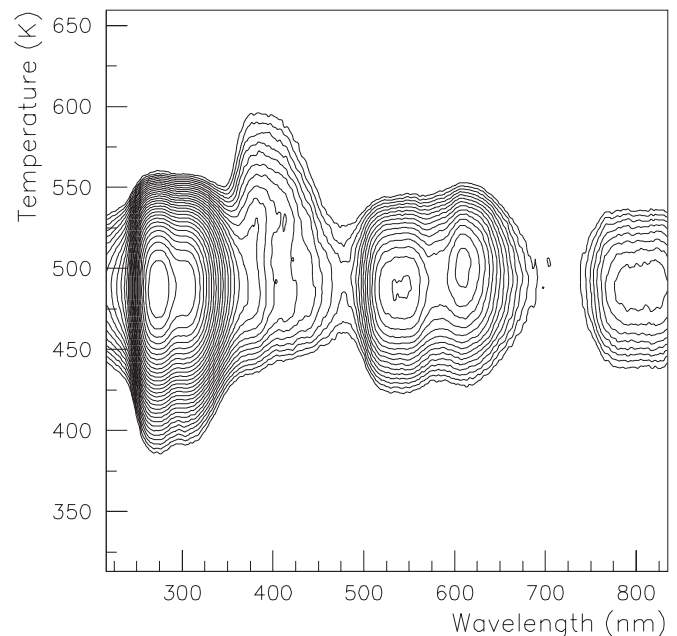


FIG. 10. Wavelength-resolved TSL measurements performed on LPS:0.5mol%Pr after RT x-ray irradiation.

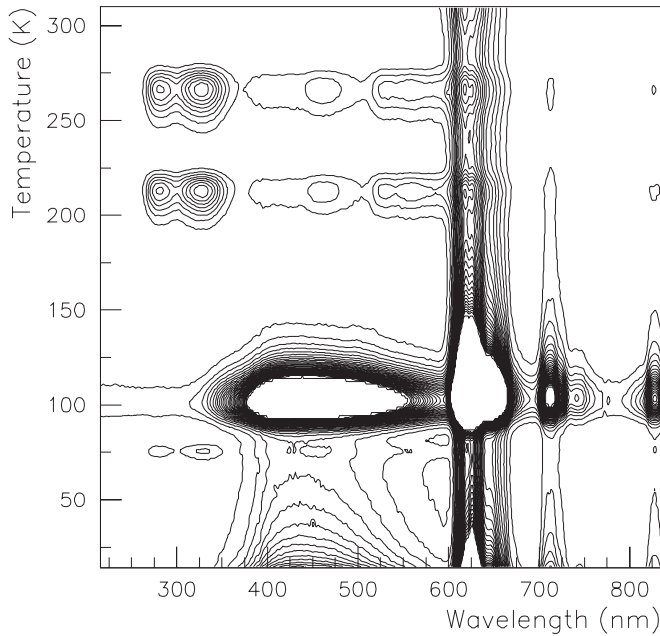


FIG. 11. Wavelength-resolved TSL measurements performed on LPS:0.5mol%Pr after x-ray irradiation at 10 K.

technique.¹⁴ The results are reported in Table I. The data are similar to those reported in Ref. 15. In that paper only one broad peak could be evidenced in the 480 K region. In this case, using light illumination, we could identify two distinct peaks at 460 and 515 K.

3. Step 3

The delayed recombination curves were fit according to Eq. (8). The decay times of each trap entering in the equation were calculated from the values of T_m and E using expression (3), where s given by

$$s = \frac{\beta E}{k_B T_m^2} e^{\frac{E}{k_B T_m}}. \quad (9)$$

Equation (9) is valid in the framework of first-order recombination kinetics, which the involved TSL peaks were shown to obey to in Ref. 15. In order to reduce the number of parameters, we chose to consider only four TSL peaks that displayed a relative higher intensity, namely those at 77, 211, 267, and 460 K.

We chose to use the following fit approach. The parameters E and T_m were fixed to the experimental values obtained from TSL. The amplitudes A_i and the ionization energy E_{th}

TABLE I. Parameters of TSL peaks recombining in the $5d_1-4f$ transition of Pr^{3+} . The error for E is $\pm 10\%$.

LPS:Pr	T_m (K)	E (eV)
LT	77 ± 2	0.19
	211 ± 2	0.53
	267 ± 2	0.80
HT	334 ± 2	0.80
	460 ± 7	1.27
	515 ± 7	1.10

were considered free parameters. In this case we experienced a substantial difficulty of obtaining fit convergence because of the high number of parameters. Therefore we moved to a semistatistical approach using *Mathematica 8.0* software: the starting values of E_{th} and of the amplitudes A_i were generated randomly and kept fixed during each fit session. As many as 10^4 sessions were performed. Selected examples of the fits are reported in Fig. 8. The values of E_{th} minimizing χ^2 were 0.42 eV and 0.54 eV for the short and the long time windows, respectively. The values obtained are consistent with those evaluated with the first method. However, we underline that the evaluation of trap parameters by TSL analysis should be carried on in an optimal way in order to obtain a reliable result. Indeed, we succeeded to reconstruct very well low T TSL peaks with the parameters obtained, while not fully satisfactory results were found for peaks above 400 K.

With respect to Method I, this second approach is certainly more complicated, since it requires more complex experiments and delicate data analyses. However, for those materials in which stable traps are absent in a convenient temperature range, it could be the only practicable route. Besides the proposed application perspectives, we believe that such a model satisfactorily shows the relationship between trapping centers, TSL-glow curves, and delayed recombination processes revealing the complicated dynamics of carrier trapping, detrapping, and recombination as a function of temperature,

IV. CONCLUSIONS

Two methods for the evaluation of the thermal ionization energy, E_{th} , of an excited state level of a RE ion in an insulating host have been described. In both cases the role of defects acting as carrier traps has been exploited. The investigation has been focused on LPS:Pr scintillator as an example.

One approach involves only TSL measurements following ultraviolet irradiation with light belonging to the excitation spectrum of the $4f-5d_1$ level at several temperatures. As it has been described, the method is relatively simple and allows a reliable evaluation of E_{th} , provided that some necessary properties of the traps employed are verified, like thermal stability in the temperature range considered and TSL emission linearity versus their filling by carriers.

The second approach consists of considering the tight correlation between delayed recombination decay related to the $5d_1-4f$ transition and defects acting as carrier traps delaying their radiative recombination. In this paper we have proposed the feasibility of a numerical reconstruction of the temperature dependence of the slow components' intensity with the sum of contributions from different traps investigated by TSL, in two different time windows.

This represents a clear and quantitative evidence of such correlation, which was proposed until now mainly in a qualitative way. Moreover, we have shown that such numerical reconstruction also allows the determination of the thermal ionization energy that can be considered as a free parameter of the fit. At variance with the first method, in this case no specific requirements for the characteristics of traps are needed. However, due to the complexity of the fit, the use of this approach requires a very careful preventive investigation of traps parameters by TSL methods. Future tests of such a

method on other materials and its comparison with different techniques will allow one to further verify its reliability.

ACKNOWLEDGMENTS

The financial support of the Italian CARIPLO Foundation project “Energy transfer and trapping processes in nanos-

structured scintillator materials” (2008–2011) of the Czech Academy of Sciences GAAV project KAN300100802 and of the MSMT KONTAKT project ME10084 are gratefully acknowledged. The authors are thankful to G. Ren from Shanghai Institute of Ceramics for providing the crystals for this study.

*mauro.fasoli@mater.unimib.it

¹P. Dorenbos, *J. Phys. Condens. Matter* **15**, 575 (2003).

²P. Dorenbos, A. H. Krumpel, E. van der Kolk, P. Boutinaud, M. Bettinelli, and E. Cavalli, *Opt. Mater.* **32**, 1681 (2010).

³N. R. J. Poolton, A. J. J. Bos, G. O. Jones, and P. Dorenbos, *J. Phys. Condens. Matter* **22**, 185403 (2010).

⁴P. Dorenbos and A. J. J. Bos, *Radiat. Meas.* **43**, 139 (2008).

⁵J. Fleniken, J. Wang, J. Grimm, M. J. Weber, and U. Happek, *J. Lumin.* **94–95**, 465 (2001).

⁶H. Loudyi, Y. Guyot, S. A. Kazanskii, J.-C. Gâcon, B. Moine, C. Pédrini, and M.-F. Joubert, *Phys. Rev. B* **78**, 045111 (2008).

⁷U. Happek, S. A. Basun, J. Choi, J. K. Krebs, and M. Raukas, *J. Alloys Compd.* **303–304**, 198 (2000).

⁸C. W. Thiel, H. Cruguel, H. Wu, Y. Sun, G. J. Lapeyre, R. L. Cone, R. W. Equall, and R. M. Macfarlane, *Phys. Rev. B* **64**, 085107 (2001).

⁹J. Pejchal, M. Nikl, E. Mihokova, A. Novoselov, A. Yoshikawa, and R. T. Williams, *J. Lumin.* **129**, 1857 (2009).

¹⁰H. Feng, V. Jary, E. Mihokova, D. Ding, M. Nikl, G. Ren, H. Li, S. Pan, A. Beitlerova, and R. Kucerkova, *J. Appl. Phys.* **108**, 033519 (2010).

¹¹D. Pauwels, N. Lemasson, B. Viana, A. Kahn-Harari, E. V. D. van Loef, P. Dorenbos, and C. W. E. van Eijk, *IEEE Trans. Nucl. Sci.* **47**, 1787 (2000).

¹²L. Pidol, B. Viana, A. Kahn-Harrari, A. Bessiere, and P. Dorenbos, *Nucl. Instrum. Methods Phys. Res. A* **537**, 125 (2005).

¹³H. Y. Li, L. S. Qin, S. Lu, and G. H. Ren, *J. Inorg. Mater.* **21**, 527 (2006).

¹⁴S. W. S. McKeever, *Thermoluminescence of Solids* (Cambridge University Press, Cambridge 1985).

¹⁵E. Mihóková, M. Fasoli, F. Moretti, M. Nikl, V. Jary, G. Ren, and A. Vedda, *Opt. Mater* **34**, 872 (2012).